# SWITCHING PAIRWISE MARKOV CHAINS FOR NON STATIONARY TEXTURED IMAGES SEGMENTATION

Mohamed El Yazid Boudaren[1], Emmanuel Monfrini[2] and Wojciech Pieczynski[2]
[1]*Ecole Militaire Polytechnique, Laboratoire Mathématiques Appliquées*
*PO Box 17, Algiers 16111, Algeria*
[2]*Institut Telecom, Telecom SudParis, CITI Dpt., CNRS UMR 5157,*
*9 rue Charles Fourier, Evry 91000, France*

**ABSTRACT**

Hidden Markov chains (HMCs) have been extensively used to solve a wide range of problems related to computer vision, signal processing (Cappé, O., et al 2005) or bioinformatics (Koski, T., 2001). Such notoriety is due to their ability to recover the hidden data of interest using the entire observable signal thanks to some Bayesian techniques like MPM and MAP. HMCs have then been generalized to pairwise Markov chains (PMCs), which offer similar processing advantages and superior modeling possibilities. However, when applied to nonstationary data like multi-textures images, both HMCs and PMCs fail to produce tolerable results given the mismatch between the estimated model and the data under concern. The recent triplet Markov chains (TMCs) have offered undeniable means to solve such challenging difficulty through the introduction of a third underlying process that may model, for instance, the switches of the model along the signal. In this paper, we propose a new TMC that incorporates a switching PMC to model non stationary images. To validate our model, experiments are carried out on synthetic and real multitextured images in an unsupervised manner.

**KEYWORDS**

Hidden Markov chains, switching pairwise Markov chains, textured image segmentation.

## 1. INTRODUCTION

The hidden Markov chains have widely been applied to various image processing problems including supervised and unsupervised image segmentation. When the image under consideration is stationary, these models are quite proficient and their corresponding unsupervised Bayesian segmentation techniques using EM (Expectation- Maximization) yield suitable results. However, when the image is nonstationary, they fail to establish a satisfactory association with the image to be modeled and the segmentation results can be relatively poor. To overcome this limitation, authors in (Lanchantin, P. et al, 2011) propose a particular TMC called switching hidden Markov chains (S-HMC) to take the switches of the model into account. In such a model, each stationary part of the image is modeled via a classical HMC and the switches between these different parts are assumed to be Markovian. The same thing happens when we consider a multi-textured image; it is intuitive to consider a HMC per each texture. Furthermore, the gain in using S-HMC is that the switches between different textures are governed by a Markov chain rather than independent on each other, which may serve as a regularization tool to prevent the "pepper and salt" aspect of the unobserved image which is being determined.

In this paper, we deal with the problem of non stationary image modeling with application to multi-textured image segmentation. For this purpose, we propose an original approach, based on a switching PMC rather than a switching HMC to model textured images. Supremacy of PMCs over HMCs has already been shown in previous works (Derrode, S. and Pieczynski, W., 2004). It hinges essentially on their ability to take complex noises into account. In particular, in PMCs, one can easily model the fact that pixels near region boundaries inside the image may have different visual aspect than those located inside region.

The remainder of this paper is organized as follows: the next section summarizes the hidden, pairwise and triplet Markov chains. The third section presents the proposed switching pairwise Markov chains.

Experimental results are provided in the fourth section. Concluding remarks and future improvements end the paper.

## 2. HIDDEN, PAIRWISE AND TRIPLET MARKOV CHAINS

In this section, we briefly describe three families of Markov chains with strictly increasing degrees of generality: HMCs, PMCs and TMCs. Let us notice that HMCs, which are the most basic ones, were extended in different directions. However, to our knowledge, in all these extensions, the hidden process remains Markovian and the resulting models are still hidden Markov models (Pieczynski, W., 2010). On the other hand, PMCs in which the hidden process is not Markovian exist and are therefore firmly more general. Similarly, TMCs form a family which is strictly more general than PMCs since TMCs that are not PMCs exist and were used to deal with several data irregularities that neither HMCs nor PMCs can handle (Boudaren, M. E. Y., et al, 2011).

All along this section, we consider an observable signal $Y = (Y_n)_{n=1}^N$ that is to be indexed into $X = (X_n)_{n=1}^N$where $Y_n$ take their values in $\mathbb{R}$ and $X_n$ take their values from a finite set of classes $\Omega = \{\omega_1, .., \omega_K\}$. Realizations of the processes will be denoted by lowercase letters. To simplify the notations, we will write $p(x_n)$ instead of $p(X = x_n)$. Accordingly, we recall the formalisms of HMCs, PMCs and TMCs.

### 2.1 Hidden Markov Chains

A HMC is a pairwise process $Z = (X, Y) = (X_n, Y_n)_{n=1}^N$that considers *X* as a Markov chain which is to be recovered from its noisy version *Y*. Moreover, when the classical noise assumptions hold, the joint probability of *Z* is given by the simple formula:

$$p(z) = p(x_1)p(y_1|x_1)\prod_{n=2}^N p(x_n|x_{n-1})\,p(y_n|x_n) \quad (1)$$

Accordingly, *X* may be recovered from *Y* by means of some Bayesian decision rules such as marginal posterior mode (MPM) or maximum a posteriori (MAP) (Rabiner, L. R., 1989). Throughout this paper, MPM will be adopted. Its corresponding formula is the following:

$$[\hat{x} = \hat{x}_{MPM}(y)] \Leftrightarrow [\hat{x}_n = argmax_{\,i}\, p(x_n = \omega_i|y)] \quad (2)$$

When the model parameters are known, the posterior distributions $p(x_n|y)$ required to perform MPM estimation are computed thanks to forward functions $\alpha_n(x_n) = p(y_1, \dots, y_n, x_n)$ and backward functions $\beta_n(x_n) = p(y_{n+1}, \dots, y_N|x_n)$ that can be computed in the following iterative way:

$$\alpha_1(x_1) = p(x_1)p(y_1|x_1);$$

$$\alpha_{n+1}(x_{n+1}) = \sum_{x_n\in\Omega} \alpha_n(x_n)p(x_{n+1}|x_n)p(y_{n+1}|x_{n+1}) \quad (3)$$

$$\beta_N(x_N) = 1;$$

$$\beta_n(x_n) = \sum_{x_{n+1}\in\Omega} \beta_{n+1}(x_{n+1})p(x_{n+1}|x_n)p(y_{n+1}|x_{n+1}) \quad (4)$$

The posterior margins can then be computed as follows:

$$p(x_n|y) \propto \alpha_n(x_n)\beta_n(x_n) \quad (5)$$

The indexing is then derived according to equation 2.

On the other hand, when the model parameters are unknown, several relatively quick algorithms can be used to find out these latter. We can cite for instance expectation- maximization algorithm (EM), its stochastic version (SEM) or iteratve conditional estimation (ICE) (Pieczynski, W., 2010).

### 2.2 Pairwise Markov Chains

*Z* is referred to as a PMC if Z is itself Markovian. Hence, Z is said to be a PMC if and only if its joint distribution is given by

$$p(z) = p(z_1)\prod_{n=2}^{N} p(z_n|z_{n-1}) \quad (6)$$

An HMC defined by (1) can then be seen as a particular PMC where $p(z_n|z_{n-1}) = p(x_n|x_{n-1})p(y_n|x_n)$ whereas in more general PMC we have$p(z_n|z_{n-1}) = p(x_n|x_{n-1}, y_{n-1})p(y_n|x_{n-1}, y_{n-1}, x_n)$. This shows the greater generality of PMC over HMC at the local level. At the global level, the noise distribution $p(y|x)$ is of Markovian form in PMC whereas it is given by the simple formula $p(y|x) = \prod_{n=1}^{N} p(y_n|x_n)$ in HMC. The posterior margins $p(x_n|y)$ required for MPM restoration are computable within linear computational complexity like for HMC thanks to the same forward functions $\alpha_n(x_n) = p(y_1, \dots, y_n, x_n)$ and extended backward functions $\beta_n(x_n) = p(y_{n+1}, \dots, y_N|x_n, y_n)$that can be computed in the following iterative way:

$$\alpha_1(x_1) = p(x_1, y_1);$$

$$\alpha_n(x_n) = \sum_{x_{n-1}\in\Omega} \alpha_{n-1}(x_{n-1})p(x_n, y_n|x_{n-1}, y_{n-1}) \quad (7)$$

$$\beta_N(x_N) = 1;$$

$$\beta_n(x_n) = \sum_{x_{n+1}\in\Omega} \beta_{n+1}(x_{n+1})p(x_{n+1}, y_{n+1}|x_n, y_n) \quad (8)$$

When the model parameters are unknown, they can be estimated via adapted variants of the same Bayesian algorithms used for HMCs. For further details, the reader may refer to (Derrode, S. and Pieczynski, W., 2004) where some related theoretical developments and experiments are shown.

## 2.3 Triplet Markov Chains

$Z$ is said to be a TMC if there exists a third process $U = (U_1, \dots, U_N)$ with each $U_n$ taking its values from a finite set $\Lambda = \{\lambda_1, \dots, \lambda_M\}$ such that the triplet $T = (X, Y, U)$ is a Markov chain. Let $V = (U, X)$. $T = (V, Y)$ is then a pairwise Markov chain (PMC). This makes the computation of the distributions $p(x_n|y)$, required to perform MPM restoration, affordable even when $Z$ is not Markovian. This shows the greater generality of TMC over PMC, which is more general than HMC.

# 3. SWITCHING PAIRWISE MARKOV CHAINS

## 3.1 The Model

Let $Y = (Y_n)_{n=1}^{N}$be an observable signal that is to be indexed into $X = (X_n)_{n=1}^{N}$where $Y_n$ are in $\mathbb{R}$ and $X_n$ belongs to $\Omega = \{\omega_1, .., \omega_K\}$. Let us consider now the situation where the data $Z = (X, Y)$ follow a pairwise Markov chain with parameters depending on the realizations of a third Markovian process $U = (U_n)_{n=1}^{N}$, where each $U_n$ belongs to $\Lambda = \{\lambda_1, \dots, \lambda_M\}$. More precisely we will assume that the transition probability of $Z$ is then given by:

$$p(z_n, u_n|z_{n-1}, u_{n-1}) = p(u_n|u_{n-1})p(x_n|x_{n-1}, y_{n-1}, u_n)p(y_n|x_{n-1}, y_{n-1}, x_n, u_n) \quad (9)$$

This gives a particular TMC that will be referred to as a switching pairwise Markov chain (S- PMC) that extends the switching hidden Markov chain (S-HMC) (Lanchantin, P. et al, 2011). The plain PMC can be seen as a particular S-PMC where we have a unique regime and thus a unique PMC without any switches. The S- PMC may then be applied to all situations where we have regime switches provided that we can model each one via a PMC.

## 3.2 Application to Textured Images Modeling

We apply now our model S-PMC to model texture images. Let us consider the most general case where the image contains more than one texture. Let $I = (I_{ab})_{a,b=1}^{h}$ be such an image where $I_{ab}$ is the pixel with position$(a, b)$and let $\Lambda = \{\lambda_1, \dots, \lambda_M\}$ be the set of M textured classes present in the image. The problem of image segmentation consists then in assigning each image pixel to one of these classes. To make our model applicable, we need first to convert the two-dimensional image $I$ into one-dimensional signal. For this

purpose we use the Hilbert-Peano scan. This gives a mono-dimensional signal $Y = (Y_n)_{n=1}^N$ that is to be indexed into $U = (U_n)_{n=1}^N$ where $Y_n$ are assumed to be real numbers and $U_n$ are in $\Lambda$. According to S-PMC formalism, we have to model each texture class $\lambda_m$ via a stationary PMC. Since we assume each mono-texture sub-image to be stationary, only stationary PMC in which $p(z_{n-1}, z_n|U_n = \lambda_m)$ does not depend on $n$ will be considered. Let us denote $p_m(i,j) = p(X_{n-1} = \omega_i, X_n = \omega_j|U_n = \lambda_m)$ and $f_m^{i,j}(y_{n-1}, y_n) = p(y_{n-1}, y_n|X_{n-1} = \omega_i, X_n = \omega_j, U_n = \lambda_m)$. The distribution of $Z$ is then given by:

$$p(z_{n-1}, z_n|U_n = \lambda_m) = p_m(i,j) f_m^{i,j}(y_{n-1}, y_n) \quad (10)$$

The distribution of the Markov chain Z can be equivalently determined by the initial probabilities $p(z_1|U_2 = \lambda_m)$ given by $p(z_1|U_2 = \lambda_m) = \sum_{\omega_j \in \Omega} p_m(i,j) \int_{\mathbb{R}} f_m^{i,j}(y_1, y_2)\, dy_2 = \sum_{\omega_j \in \Omega} p_m(i,j) f_m^{i,j}(y_1)$ and the transition matrix given by $p(z_n|z_{n-1}, U_n = \lambda_m) = \frac{p(z_{n-1}, z_n|U_n = \lambda_m)}{p(z_{n-1}|U_n = \lambda_m)} = \frac{p_m(i,j) f_m^{i,j}(y_{n-1}, y_n)}{\sum_{\omega_j \in \Omega} p_m(i,j) f_{i,j}(y_{n-1})}$.

In this work, only Gaussian S-PMC will be considered. An S-PMC is called Gaussian if and only if all its densities $f_m^{i,j}$ are Gaussian. Hence, an S-PMC $Z$ can be specified through the transition matrix $\mathrm{A} = (a_{\lambda,\lambda'})$ where $a_{\lambda,\lambda'} = p(U_n = \lambda'|U_{n-1} = \lambda)$, the $M$ matrices $\Gamma_m = (\gamma_m^{i,j})$ where $\gamma_m^{i,j} = p_m(i,j)$ and the means $\mu_{m,1}^{i,j}, \mu_{m,2}^{i,j}$, the standard deviations $\sigma_{m,1}^{i,j}, \sigma_{m,2}^{i,j}$ and the correlation coefficient $\rho_m^{i,j}$ of the $M \times K^2$ bi-dimensional densities $f_{i,j}$.

## 3.3 Bayesian MPM Segmentation of a Textured Image

To accomplish the segmentation $\hat{u}$ of the image $I$, one has to compute the marginal distributions $p(u_n|y)$. When the parameters of the model are given, the posterior marginal distributions $p(u_n, x_n|y)$ are workable via the forward function $\alpha_n(v_n) = p(y_1, \dots, y_n, v_n)$ and extended backward one $\beta_n(x_n) = p(y_{n+1}, \dots, y_N|v_n, y_n)$ that may be computed in the following iterative way:

$$\alpha_1(v_1) = p(v_1, y_1);$$

$$\alpha_n(v_n) = \sum_{v_{n-1} \in \Lambda \times \Omega} \alpha_{n-1}(v_{n-1}) p(u_n|u_{n-1}) p(z_n|z_{n-1}, u_n) \quad (11)$$

$$\beta_N(v_N) = 1;$$

$$\beta_n(v_n) = \sum_{v_{n+1} \in \Lambda \times \Omega} \beta_{n+1}(v_{n+1}) p(u_n|u_{n-1}) p(z_{n+1}|z_n, u_{n+1}) \quad (12)$$

The posterior distributions of $V$ and $U$ can then be derived as follows:

$$p(v_n|y) \propto \alpha_n(v_n) \beta_n(v_n) \quad (13)$$

$$p(u_n|y) = \sum_{x_n \in \Omega} p(v_n|y) \quad (14)$$

## 3.4 Parameters Estimation

When the model parameters $\Theta = (\mathrm{A}, \Gamma_m, \mu_{m,1}^{i,j}, \mu_{m,2}^{i,j}, \sigma_{m,1}^{i,j}, \sigma_{m,2}^{i,j}, \rho_m^{i,j})$ are unknown, we propose to estimate them using the EM iterative algorithm according to the following steps:

i) Choose an initial set of parameters $\Theta^0 = (\mathrm{A}, \Gamma_m, \mu_{m,1}^{i,j}, \mu_{m,2}^{i,j}, \sigma_{m,1}^{i,j}, \sigma_{m,2}^{i,j}, \rho_m^{i,j})^0$.

ii) For each iteration, we compute $\psi_n(v_n, v_{n+1}) = p(v_n, v_{n+1}|y)$ and $\xi_n(v_n) = p(v_n|y)$ according to $\Theta^q$ thanks to:

$$\psi_n(v_n, v_{n+1}) \propto \alpha_n(v_n) a_{u_n, u_{n+1}} p(z_{n+1}|z_n, u_{n+1}) \beta_{n+1}(v_{n+1}) \quad (15)$$

$$\xi_n(v_n) = \sum_{v_{n+1}} \psi_n(v_n, v_{n+1}) \quad (16)$$

Then we derive $\Theta^{q+1}$ as follows

$$\left(\mu_{m,1}^{i,j}\right)^{q+1} = \frac{\sum_{n=1}^{N-1}\sum_{v_n,v_{n+1}}\psi_n(v_n,v_{n+1})y_n 1_{\left[(u_n,x_n,x_{n+1})=\left(\lambda_m,\omega_i,\omega_j\right)\right]}}{\sum_{n=1}^{N-1}\sum_{v_n,v_{n+1}}\psi_n(v_n,v_{n+1})1_{\left[(u_n,x_n,x_{n+1})=\left(\lambda_m,\omega_i,\omega_j\right)\right]}} \quad (17)$$

$$\left(\mu_{m,2}^{i,j}\right)^{q+1} = \frac{\sum_{n=1}^{N-1}\sum_{v_n,v_{n+1}}\psi_n(v_n,v_{n+1})y_{n+1} 1_{\left[(u_n,x_n,x_{n+1})=\left(\lambda_m,\omega_i,\omega_j\right)\right]}}{\sum_{n=1}^{N-1}\sum_{v_n,v_{n+1}}\psi_n(v_n,v_{n+1})1_{\left[(u_n,x_n,x_{n+1})=\left(\lambda_m,\omega_i,\omega_j\right)\right]}} \quad (18)$$

$$\left(\sigma_{m,1}^{i,j}\right)^{q+1} = \frac{\sum_{n=1}^{N-1}\sum_{v_n,v_{n+1}}\psi_n(v_n,v_{n+1})\left(y_n-\left(\mu_{m,1}^{i,j}\right)^{q+1}\right)^2 1_{\left[(u_n,x_n,x_{n+1})=\left(\lambda_m,\omega_i,\omega_j\right)\right]}}{\sum_{n=1}^{N-1}\sum_{v_n,v_{n+1}}\psi_n(v_n,v_{n+1})1_{\left[(u_n,x_n,x_{n+1})=\left(\lambda_m,\omega_i,\omega_j\right)\right]}} \quad (19)$$

$$\left(\sigma_{m,2}^{i,j}\right)^{q+1} = \frac{\sum_{n=1}^{N-1}\sum_{v_n,v_{n+1}}\psi_n(v_n,v_{n+1})\left(y_{n+1}-\left(\mu_{m,2}^{i,j}\right)^{q+1}\right)^2 1_{\left[(u_n,x_n,x_{n+1})=\left(\lambda_m,\omega_i,\omega_j\right)\right]}}{\sum_{n=1}^{N-1}\sum_{v_n,v_{n+1}}\psi_n(v_n,v_{n+1})1_{\left[(u_n,x_n,x_{n+1})=\left(\lambda_m,\omega_i,\omega_j\right)\right]}} \quad (20)$$

$$\left(\rho_{m}^{i,j}\right)^{q+1} = \frac{\sum_{n=1}^{N-1}\sum_{v_n,v_{n+1}}\psi_n(v_n,v_{n+1})\left(y_n-\left(\mu_{m,1}^{i,j}\right)^{q+1}\right)\left(y_{n+1}-\left(\mu_{m,2}^{i,j}\right)^{q+1}\right)1_{\left[(u_n,x_n,x_{n+1})=\left(\lambda_m,\omega_i,\omega_j\right)\right]}}{\sum_{n=1}^{N-1}\sum_{v_n,v_{n+1}}\psi_n(v_n,v_{n+1})1_{\left[(u_n,x_n,x_{n+1})=\left(\lambda_m,\omega_i,\omega_j\right)\right]}} \quad (21)$$

$$a_{l,m}^{q+1} = \frac{\sum_{n=1}^{N-1}\sum_{v_n}\psi_n(v_n,v_{n+1})1_{[(u_n,u_{n+1})=(\lambda_l,\lambda_m)]}}{\sum_{n=1}^{N-1}\sum_{v_n}\xi_n(v_n)1_{[u_n=\lambda_l]}} \quad (22)$$

$$\left(\gamma_{m}^{i,j}\right)^{q+1} = \frac{\sum_{n=1}^{N-1}\sum_{v_n}\psi_n(v_n,v_{n+1})1_{\left[(u_{n+1},x_n,x_{n+1})=\left(\lambda_m,\omega_i,\omega_j\right)\right]}}{\sum_{n=1}^{N-1}\sum_{v_n}\xi_n(v_n)1_{[u_{n+1}=\lambda_m]}} \quad (23)$$

iii) We repeat the previous step until an end criterion is reached.

# 4. EXPERIMENTS

In this section, we present three series of experiments. In the first one, synthetic textured images are considered and MPM segmentation is achieved in an unsupervised manner via EM algorithm according to S-HMC and S-PMC proposed here. In the second set of experiments, we judge our model via experiments conducted on one Brodatz texture image (Brodatz, P., 1966). In the last set of experiments, we consider an assorted image that we assembled by combining some mono-class texture images from CGT database. All along this section, one-dimensional chains are converted to and from 2D images using the Hilbert-Peano scan.

## 4.1 Unsupervised Segmentation of Synthetic Textured Images

For this set of experiments, we will consider two real classes $\Omega = \{\omega_1, \omega_2\}$ and three texture classes $\Lambda = \{\lambda_1, \lambda_2, \lambda_3\}$. Textures images of size $128 \times 128$ are generated according to S-PMC formalism as follows: $U = u$ realization sequence is fixed in the following manner: pixels of the image upper left quarter are assigned to $\lambda_1$(black), pixels of the second quarter are assigned to $\lambda_2$ (grey) and pixels of the last half are assigned to $\lambda_3$ (white). The realizations $X = x$ and $Y = y$ are simulated from $\Omega = \{\omega_1, \omega_2\}$ (where $\omega_1$ is depicted in black and $\omega_2$ in white) and $\mathbb{R}$ according to the matrices $(\Gamma_m)_{m=1}^3$ and the noise parameters as described in section 3. The parameters used for experiments 1, 2 and 3 are given in Tables 1, 2 and 3 respectively. The corresponding segmentation results are provided in Table 4.

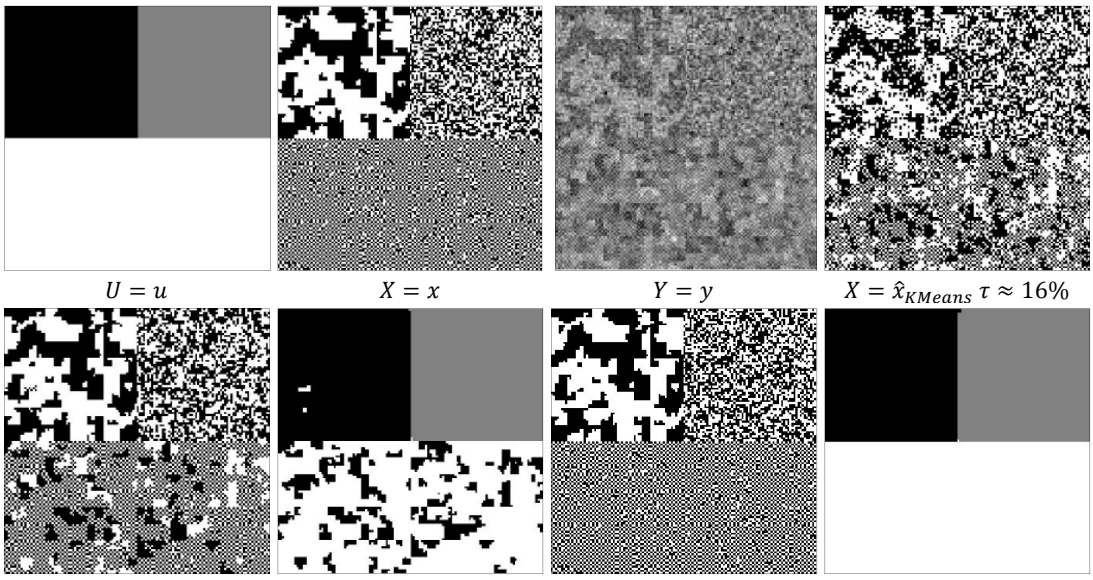


Figure 1. Unsupervised segmentation of a synthetic image from experiment 2 according to different models.

Table 1. Parameters of experiment 1

| Texture | Γ | $\mu_1$ | $\mu_2$ | $\sigma_1$ | $\sigma_2$ | $\rho$ |
|---|---|---|---|---|---|---|
| $\lambda_1$ | [0.49 0.01; 0.01 0.49] | [1 1; 3 3] | [1 3; 1 3] | [1 1; 1 1] | [1 1; 1 1] | [0 0; 0 0] |
| $\lambda_2$ | [0.25 0.25; 0.25 0.25] | [1 1; 3 3] | [1 3; 1 3] | [1 1; 1 1] | [1 1; 1 1] | [0 0; 0 0] |
| $\lambda_3$ | [0.01 0.49; 0.49 0.01] | [1 1; 3 3] | [1 3; 1 3] | [1 1; 1 1] | [1 1; 1 1] | [0 0; 0 0] |

Table 2. Parameters of experiment 2

| Texture | Γ | $\mu_1$ | $\mu_2$ | $\sigma_1$ | $\sigma_2$ | $\rho$ |
|---|---|---|---|---|---|---|
| $\lambda_1$ | [0.49 0.01; 0.01 0.49] | [1 1; 3 3] | [1 3; 1 3] | [1 1; 1 1] | [1 1; 1 1] | [0.1 0.1; 0.1 0.1] |
| $\lambda_2$ | [0.25 0.25; 0.25 0.25] | [1 1; 3 3] | [1 3; 1 3] | [1 1; 1 1] | [1 1; 1 1] | [0.5 0.5; 0.5 0.5] |
| $\lambda_3$ | [0.01 0.49; 0.49 0.01] | [1 1; 3 3] | [1 3; 1 3] | [1 1; 1 1] | [1 1; 1 1] | [0.9 0.9; 0.9 0.9] |

Table 3. Parameters of experiment 3

| Texture | Γ | $\mu_1$ | $\mu_2$ | $\sigma_1$ | $\sigma_2$ | $\rho$ |
|---|---|---|---|---|---|---|
| $\lambda_1$ | [0.49 0.01; 0.01 0.49] | [1 1; 3 3] | [1 3; 1 3] | [1 1; 1 1] | [1 1; 1 1] | [0.5 0.5; 0.5 0.5] |
| $\lambda_2$ | [0.25 0.25; 0.25 0.25] | [2 2; 4 4] | [2 4; 2 4] | [1 1; 1 1] | [1 1; 1 1] | [0.5 0.5; 0.5 0.5] |
| $\lambda_3$ | [0.01 0.49; 0.49 0.01] | [0 0; 2 2] | [0 2; 0 2] | [1 1; 1 1] | [1 1; 1 1] | [0.5 0.5; 0.5 0.5] |

The interest of the first experiment is to check whether the proposed S-PMC performs well when the data are generated according to an S-HMC. As shown in Table 4, the answer is affirmative; this permits to confirm that S-PMC generalizes S-HMC. The aim of the next experiments is to provide examples of situations where the former S-HMC is not suitable. In experiment 2, synthetic texture classes are governed by different transition matrices and noise correlation coefficients. In experiment 3, textures have different transition matrices and means values but the same covariance matrix. As illustrated in Table 4 and Fig. 1, the S-PMC yields significant gain in segmentation accuracy.

Table 4. Misclassification rates of synthetic textured images using different Markov chains models

| Experiment | | KMeans | S − HMC | S − PMC |
|---|---|---|---|---|
| 1 | $\tau_X$ | 15.26 | 4.58 | 4.61 |
| | $\tau_U$ | - | 0.00 | 0.00 |
| 2 | $\tau_X$ | 15.93 | 10.95 | 3.58 |
| | $\tau_U$ | - | 10.96 | 0.00 |
| 3 | $\tau_X$ | 22.75 | 17.03 | 13.25 |
| | $\tau_U$ | - | 3.83 | 0.00 |

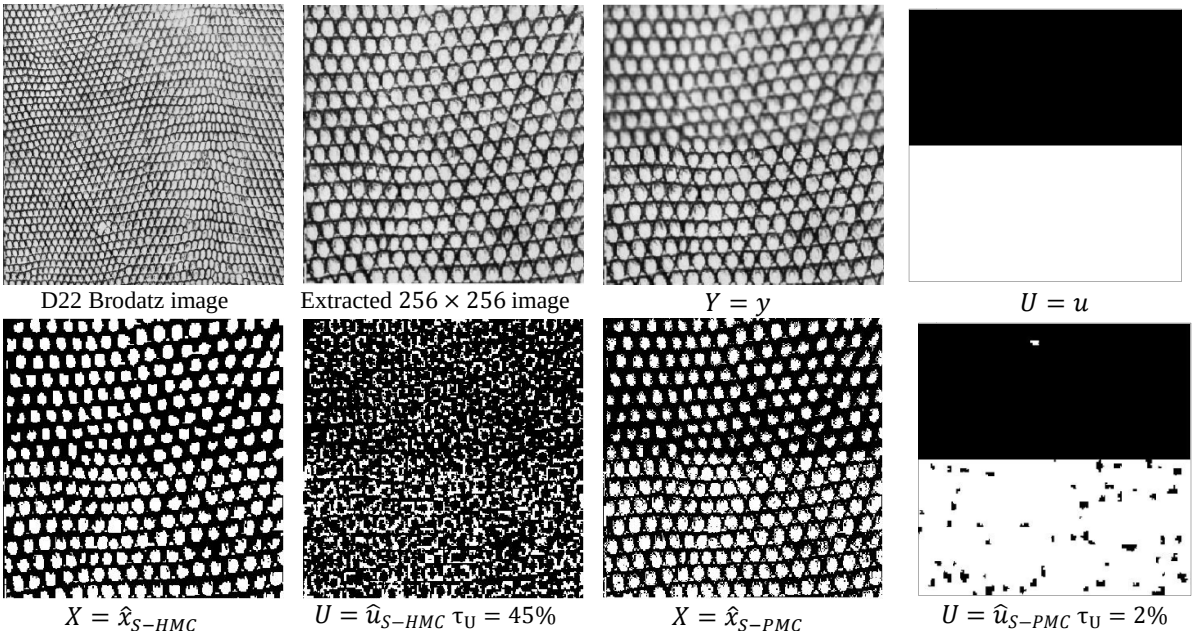


Figure 2. EM-MPM segmentation of D22 texture image according to S-HMC and S-PMC models.

## 4.2 Unsupervised Segmentation of Textured Images hidden with Average Filter

For this experiment, we consider the D22 texture image of Brodatz album from which we extract a sub-image of size $256 \times 256$. Then, we apply an average filter on the upper half of the image, which gives two stationary parts (Fig. 2). We perform then MPM-EM unsupervised segmentation according to both S-HMC and S-PMC formalisms. For both models, we consider two real classes $\Omega = \{\omega_1, \omega_2\}$ and two texture classes $\Lambda = \{\lambda_1, \lambda_2\}$. The obtained results are shown in Fig.2.

The segmentation results confirm the ability of S-PMC to take more complex noises into account. This latter property is of crucial importance since it permits to distinguish between two stationary parts of the same texture and having almost the same visual aspect.

## 4.3 Unsupervised Segmentation of Mosaic Textured Images

For this experiment, we consider an assorted textured image that we assembled using four different mono-textured images from CGT database (Fig. 3). Segmentation is achieved through MPM-EM according to both S-PMC and S-HMC models where $\Omega = \{\omega_1, \omega_2, \omega_3\}$ and four texture classes $\Lambda = \{\lambda_1, \lambda_2, \lambda_3, \lambda_4\}$.

As shown in Fig. 3, the segmentation results demonstrate the supremacy of S-PMC over S-HMC when applied to images presenting different texture classes. In fact, as shown in Fig. 3, S- PMC allows to satisfactorily recover the auxiliary process realization $U = u$ ($\tau_U = 2\%$) whereas S-HMC confounds textures $\lambda_2$(dark grey) and $\lambda_4$(white). This is due to the fact that these latter present analogous visual aspects. Hence, noise correlation represents an important complementary feature that permits to discriminate similar texture classes that classical models fail to differentiate.

# 5. CONCLUSION

In this work, we have proposed an original model designed for textured images segmentation. Our main contribution was to extend the recent switching- HMC by substituting the PMC model for the classical HMC. This extension offers more modeling potential while the parameters estimation and MPM restoration remain workable via some Bayesian methods. The efficiency of our new model was assessed against the former one

via some experiments conducted on synthetic and real texture images. It turned out that the S-PMC yields better segmentation results. As perspectives, let us cite two promising directions for further improvements. We may mention the use of the Markov fields instead of the Markov chains, which seems promising according to some preliminary results given in (Benboudjema, D., and Pieczynski, W., 2007). Another direction may concern the family of Markov trees, which can be applied to image segmentation, in particular when multiresolution images are concerned (Bouman, C., and Shapiro, M., 1994).

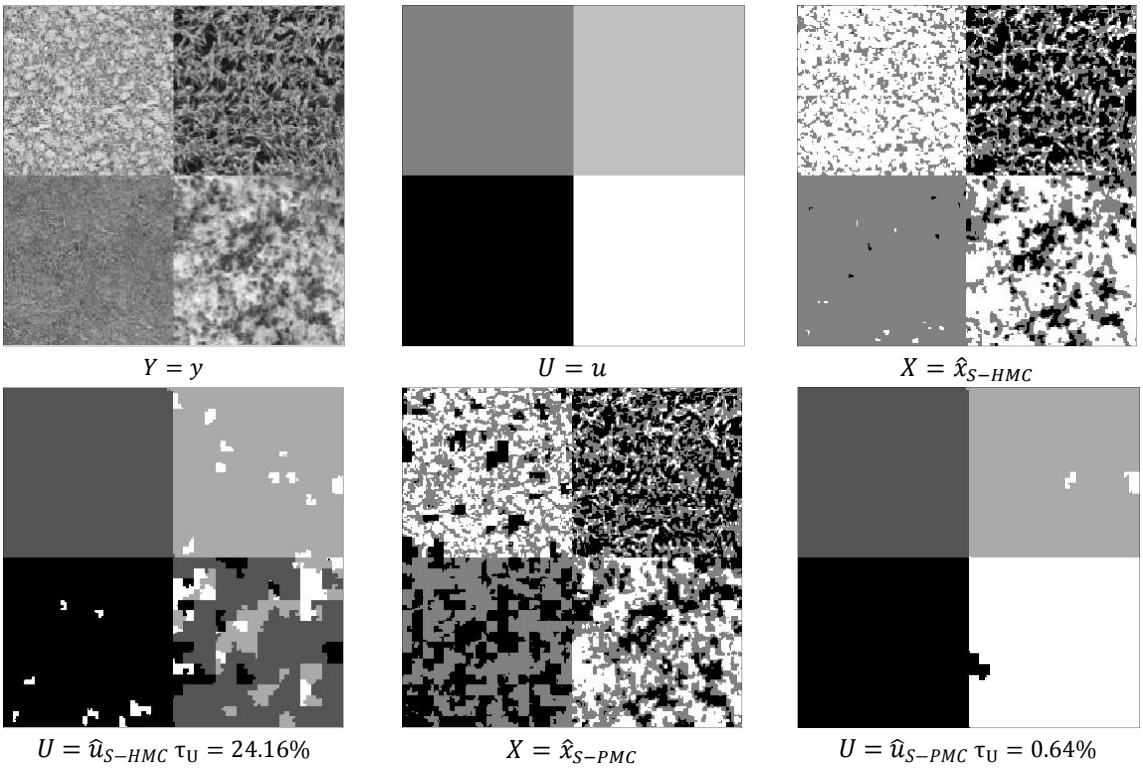


Figure 3. EM-MPM segmentation of assembled textured image according to S-HMC and S-PMC models.

## REFERENCES

Benboudjema, D. and Pieczynski, W., 2007. Unsupervised statistical segmentation of non stationary images using triplet Markov fields, *IEEE Trans. on Pattern Analysis and Machine Intelligence*, Vol. 29, No. 8, pp. 1367-1378.

Boudaren, M. E. Y., et al, 2011. Unsupervised Segmentation of Non Stationary Data Hidden with Non Stationary Noise, *Proceedings of IEEE Workshop on Systems, Signal Processing and their Applications*, Tipaza (to appear).

Bouman, C., and Shapiro, M., 1994. A Multiscale Random Field Model for Bayesian Image Segmentation. *In IEEE Transactions on Image Processing*, Vol. 3, No. 2, pp. 162- 177.

Brodatz, P., 1966. A Photographic Album for Artists and Designers. *Textures*, Dover Publications, New York.

Cappé, O., et al, 2005. Inference in hidden Markov models, Springer, New York.

Derrode, S. and Pieczynski, W., 2004. Signal and image segmentation using Pairwise Markov chains. *In IEEE Transactions on Signal Processing*, Vol. 52, No. 9, pp. 2477-2489.

Koski, T., 2001. Hidden Markov Models for Bioinformatics, Kluwer Academic Publishers.

Lanchantin, P. et al, 2011. Unsupervised segmentation of randomly switching data hidden with non-Gaussian correlated noise, *Signal Processing*, Vol. 91, No. 2, pp. 163-175.

Pieczynski, W., 2010. Triplet Markov chains and image segmentation. *In Inverse problems in Vision and 3D Tomography*, Chapter 4, A. Mohammed-Djafari ed., Wiley.

Rabiner, L. R., 1989. A tutorial on hidden Markov models and selected applications in speech recognition. *In Proceedings of IEEE*, vol. 77, no. 2, pp. 257-286.